Topography estimation in W Antarctica using level 2 radar altimeter data products

Mark Stenoien, and Charles R. Bentley
Geophysical and Polar Research Center, Department of Geology and Geophysics, University of Wisconsin-Madison. 1215 W. Dayton St, Madison WI, 53706-1692, USA

stenoien geology.wisc.edu , bentley geology.wisc.edu

URL: http://geology.wisc.edu

Abstract:

A method is presented for quickly estimating slope-corrected ice-sheet topographies directly from retracked radar altimeter surface-height estimates (i.e. from level-2 radar altimeter data products), without an intermediate slope-estimation step. The accuracy of this method is analytically evaluated for a sloped planar ice-sheet surface, and evaluated using synthetically-derived altimeter data for more complex surface topographies. Topographic maps of the Pine Island Glacier and Thwaites Glacier catchment area created by this method display a curious terrace-like quality in some regions. Comparison of these heights to aneroid-altimeter measurements collected during an over-snow traverse of the region suggest that these are real features of the ice sheet.

Keywords: radar altimeter, ice sheet, topographic estimation

1 Introduction

It is well established that ice-sheet topography has an important influence on radar-altimeter observations [Brenner et al., 1983].

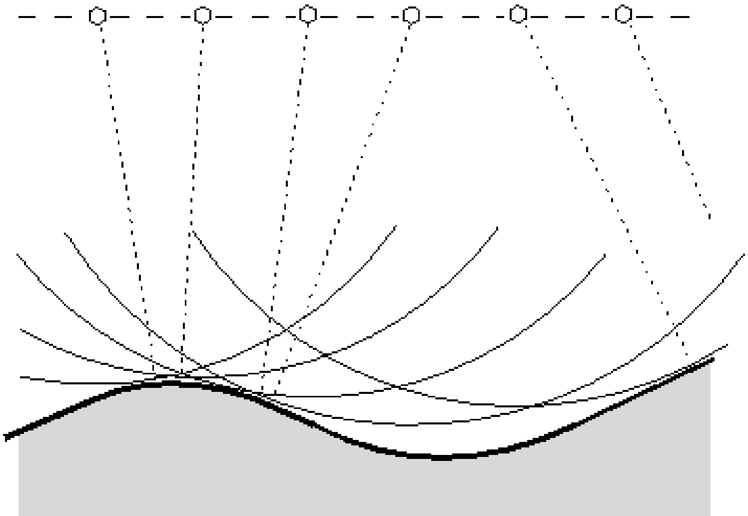

Figure 1: *The altimeter measures the distance between the satellite position (small hexagons) and the closest point on the ice surface. Because the ice-sheet is not ``flat'', the altimeter reports the range to an unknown location on the ice surface, uphill from nadir.*

Figure 1 illustrates an ice surface being interrogated by the altimeter at several different locations. The ellipses correspond to the pulse wavefront at the instant the pulse is reflected from the ice surface. The delay associated with each of these pulses is interpreted as the range between the altimeter and an unknown location on the ice surface. This location depends on the slope of the surface being observed, tending to migrate ``uphill'' from nadir. Hence, using the retracked altimeter observations ``as is'' in applications such as detecting changes in surface height requires a set of severe assumptions whose validity is difficult to prove: that the altimeter platform has traveled a orbital path in the later epoch that is sufficiently close to the path in the earlier epoch, and that no change in the surface topography has occurred between the two measurement times.

The alternative to these assumptions is to estimate the ice-sheet topography with sufficient precision that the assumptions of exactly repeating orbits and of unchanged topography are no longer necessary. Moreover, the resulting digital elevation model (DEM) is most useful for removing the elevation dependence present when using interferometric-SAR to estimate ice velocities.

2 Topographic Estimation Research

2.1 Altimeter Data Simulator

To facilitate a comparison of algorithms for topographic estimation, we have constructed a simulator that, given a description of a hypothetical snow surface in the form of coefficients for a two-dimensional Fourier Series, produces a sequence of (noisy) level-2 altimeter observations for a hypothetical altimeter mission. Since the ellipsoidal height of any portion of the hypothetical surface is known by hypothesis, competing algorithms for estimating topography can be compared to one another, according to how well they reproduce the known topography. This method has been used to evaluate the following topographic estimation technique.

2.2 Baseline Algorithm for Topographic Estimation

Our baseline, or fundamental, algorithm for topographic estimation produces a gridded estimate of topography directly from the level-2 altimeter product. This approach is seen as a less complex alternative to algorithms that apply seismic migration techniques to the waveform product [Wingham et al., 1993].

The usual first step for producing a topographic data product from a level-2 data product is to ``slope-correct'' the observations using slope information obtained from some other source, perhaps from the ensemble of altimeter data [Bamber, 1994], and then to interpolate these slope-corrected data so that height values are defined on a grid.

In contrast, the algorithm described here estimates the gridded data product directly from the level-2 altimeter data, and can be thought of as an implementation of ``3D migration'' applied to level-2 data.

We define our grid by lines of constant longitude and lines of constant latitude, (the approach is easily modified for any tesselation) spaced to produce grid nodes approximately 2 km apart. The altimeter data near each of these nodes are examined to find the return that, if it were produced by an echo originating at that node, would correspond the lowest apparent ice-surface height. Figure 2 illustrates (in two dimensions) the scalloped surface that is implied by this procedure. If altimeter observations are sufficiently dense over this neighborhood, the version of this scalloped surface sampled at the grid nodes would suffice for a biased estimate of the topography.

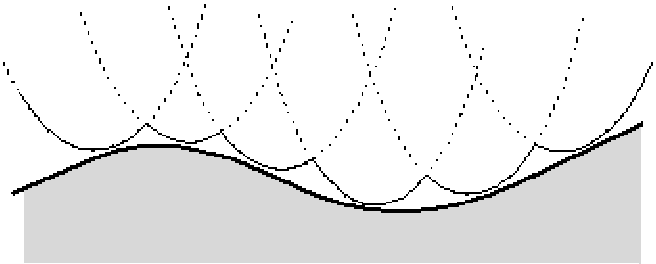

Figure 2: *The topographic estimation algorithm estimates a sampled version of the scalloped surface corresponding to the maximum feasible height of the ice-sheet given the altimeter observations (thin solid line).*

The accuracy of the approach depends on each grid point having an altimeter measurement that has interrogated a point on the ice surface (here called the *echo-point*) sufficiently close to that grid point. Hence, the more dense the altimeter observations, the better. Figure 3 shows the height-estimation error ϵ that results when the echo point and the grid point do not coincide.

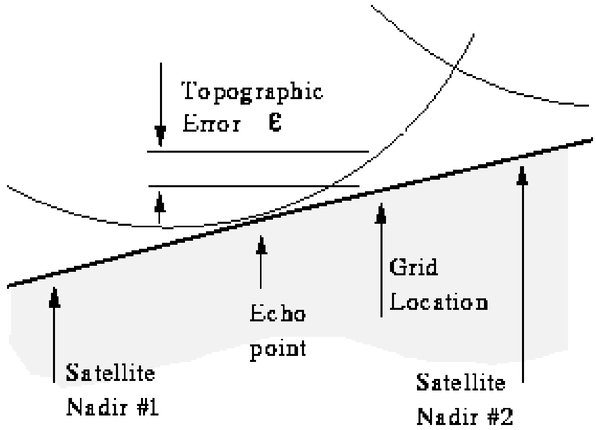

Figure 3: *Height-estimation error, ϵ that results when the echo point and the grid location do not coincide. In this picture, the topographic error is made larger by the non-zero surface slope.*

For a flat, level ice surface, the elevation error produced by this procedure at a particular grid node depends on the distance between that node and the (unknown) echo point. In the case where echo points themselves form a two-dimensional grid, as in Figure 4, where satellite tracks are spaced by distance 2*b*, consecutive along-track echo points are spaced by distance 2*a*, and the orbit height is *B*, we find that the expected error is $\frac{a^2+b^2}{6B}$, with variance $\frac{a^4+b^4}{45B^2}$, assuming the grid point falls randomly within the rectangular region between the grid points.

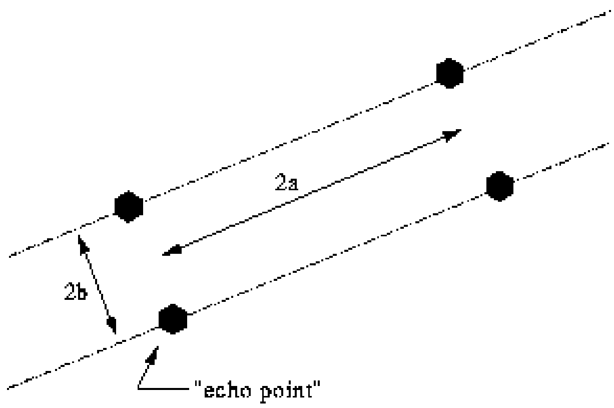

Figure 4: *Assumed geometry for the error prediction model (plan view): Echo points are spaced by distances 2a and 2b, and the satellite height is B.*

For the ERS-1 Level-2 ``ice mode'' altimeter data, $2a \approx 750$ m, the tracks are separated by a distance that depends on latitude:

$$2b \approx D\cos(90^\circ \frac{\mathrm{latitude}}{81.5^\circ})$$

where *D* is the track separation at the equator. Table 1 summarizes this ``geometric'' error behavior of the baseline algorithm.

lat.	repeat period	track sep. (m)	mean ε (m)	s.d. ε (m)
-74°	35 days	11,500	6.9	6.13
	168 days	2,400	0.33	0.27
-79°	35 days	3,800	0.8	0.69
	168 days	795	0.06	0.04

Table 1: *Theoretical performance of the baseline topography algorithm at two different latitudes. 79°S is the southern limit of the view of the SAR sensor, and 74°S is the northern limit of our region of study in West Antarctica.*

The altimeter data simulator described above can be used to compare topographies generated using the baseline algorithm to a-priori known topographies that are more complex than the tilted plane assumed above. In Figure 5, the topography used to generate a set of synthetic altimeter data is compared to a topographic estimate produced by the baseline algorithm. The synthetic altimeter data simulate a single 35-day cycle of multi-disciplinary phase data collection. This test case illustrates that a single cycle of multi-disciplinary-phase data does not produce satisfactory results with our algorithm even at 79°S.

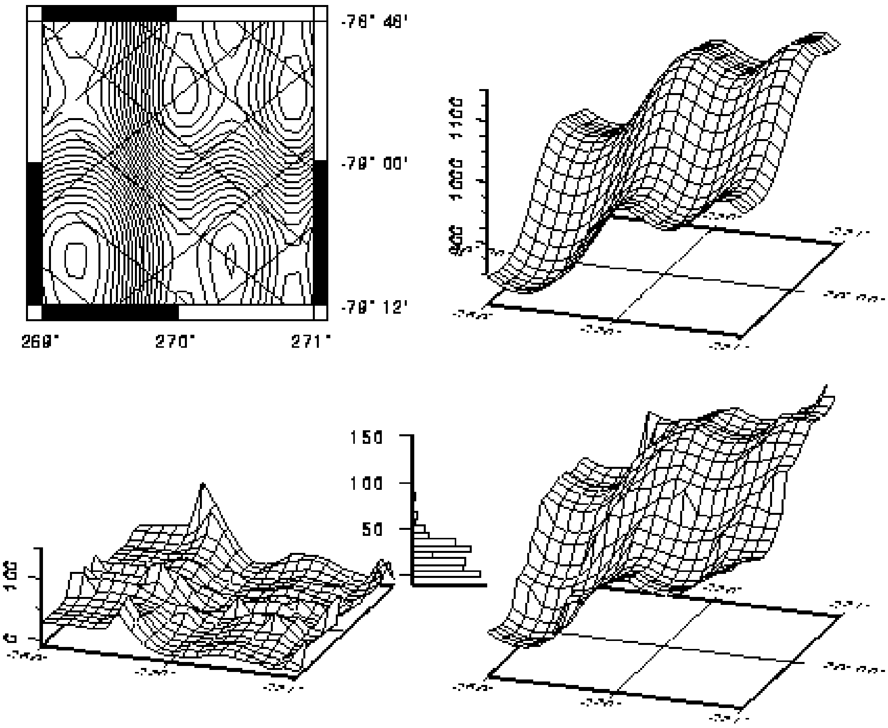

Figure 5: *Error behavior of the baseline algorithm, part 1. Upper Left: Contour plot of hypothesized ice surface, and tracks followed by the satellite nadir. Upper right: Hypothesized ice surface. Lower Right: Topographic estimate of the hypothesized ice surface produced by the baseline algorithm. Lower Left: Difference between estimate and hypothesized ice surfaces. Small histogram shows the distribution of the errors. All vertical scales have units of meters.*

Another important factor determining the accuracy of the baseline algorithm is illustrated in Figure 6. This Figure shows the topographic estimate produced using a single 168-day cycle of geodetic-phase data synthesized for the same hypothesized ice surface in Figure 5.

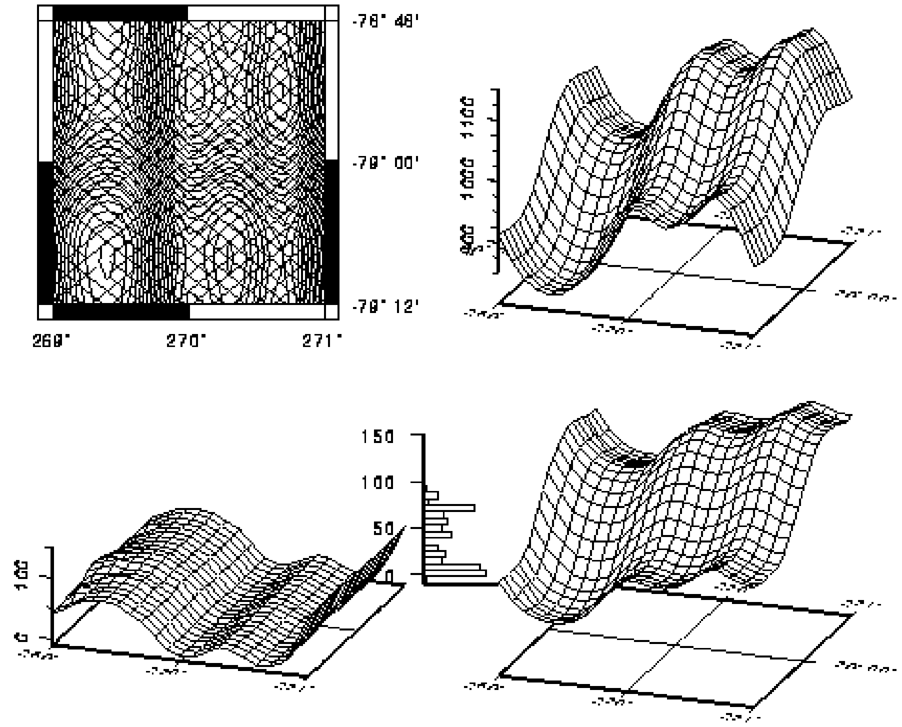

Figure: *Error behavior of the baseline algorithm, part 2. Graphs as in figure 5.*

Here the principal source of error is due to the radar altimeter's inability to ``see'' to the bottom of the troughs located at 269.8° and 270.5° longitude, since the curvature of the ice surface exceeds the curvature of the radar altimeter's wavefront. This is a well known limitation of all height estimation algorithms that use retracked altimeter data. The large error at 271° longitude results from the lack of altimeter samples interrogating that part of the ice surface; The echo points for that area have moved ``uphill'', leaving none near the edge of the test region.

In the following two sections, we discuss modifications to the baseline algorithm that either help to mitigate the effect of noisy height estimates, or decrease the geometric error.

Dimple-Filter Modification

A significant improvement to the baseline algorithm results from recording which altimeter-height datum has determined the estimate of the ice-surface height at each grid node. If some error in either the altimeter or the retracker has caused a height estimate to be anomalously low, that height estimate will determine the maximum feasible ice-sheet height over a disproportionately large area, causing the surface height estimated for many grid nodes to be determined by this one altimeter observation. When a topographic map is produced from a data set with this type of noise present, the result is a series of bowl or dimple-like depressions in the indicated surface. The so-called *dimple-filter* eliminates from the data set any altimeter datum that determines ``too many '' grid node heights, and the topography in that neighborhood is estimated again. This procedure is repeated until no altimeter datum determines ``too many'' grid node elevations. Figure 7 shows the action of this modification on a set of real altimeter data containing noisy altimeter samples.

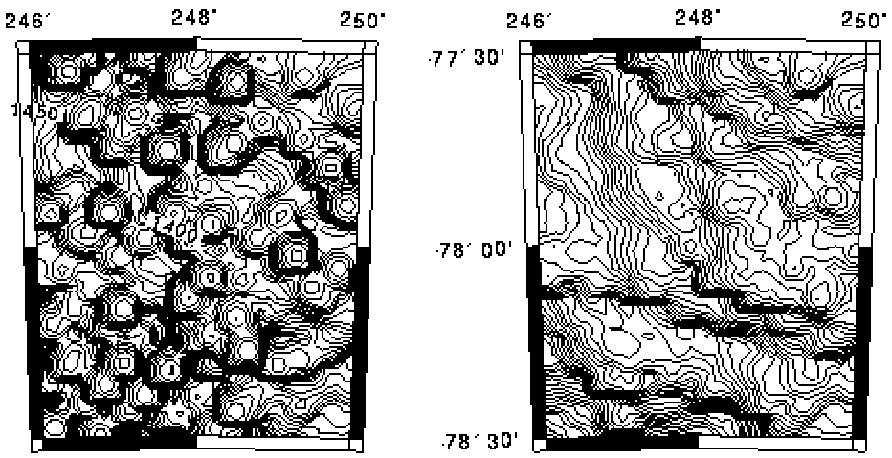

Figure 7: *Before (left), and after (right) the application of the dimple filter to an altimeter derived topography. (5m contour lines, map scale: 1:2000000)*

This Figure illustrates that a surface topography estimate produced by the unmodified baseline algorithm can easily be dominated by a small number of anomalously low surface-height readings.

Planar-facet Modification

A modification has been developed to improve the performance of the baseline algorithm on ``sparse'' data sets - that is, data sets composed of multidisciplinary phase (35-day repeat) observations, or observations from lower latitudes, where the inter-track distances are necessarily larger than a few kilometers: For each grid location where a topographic height estimate is desired, the *planar-facet* modification finds the plane tangent to the three nearest (non-colinear) lobes of the scalloped surface. The height of this plane at the grid location is used as the surface height estimate.

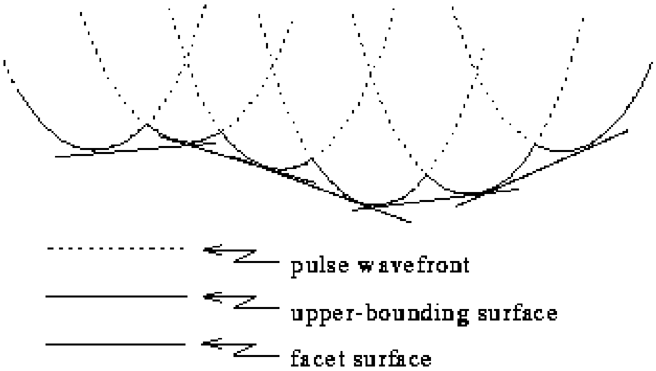

Figure 8: *The Planar-facet Modification estimates surface height at a grid node using a plane tangent to the three nearest lobes in the maximum feasible surface height.*

This procedure is depicted in Figure 8.

The planar-facet modification therefore interprets the ice surface as a collection of triangular planar-facets forming a continuous surface.

Research Activities using the ERS-1 Radar Altimeter

The radar altimeter (RA) data employed in the following sections have been upgraded and archived by Hughes STX Corporation, under contract to NASA. The data supplied by Hughes STX consisted of the ALT-WAP waveform product supplied by ESA, with precise orbit corrections based on the JGM-3 gravity model, and retracked using ``version 3'' of the 5 or 9 parameter NASA waveform retracking algorithm [Martin et al., 1983, Zwally et al., 1989].

A database has been constructed containing all retracked ERS-1 altimeter data available from Hughes STX, for the region between 80° and 170° West longitude, and 72.5° and 81.5° South latitude. This database covers several areas of glaciological interest, including the region of the Ross Ice Shelf surrounding Roosevelt Island, a large portion of Ice Stream D, all of Ice Stream E, and a large portion of the catchment areas for Thwaites and Pine Island Glaciers.

We have applied our topographic estimation algorithm to data for the region that includes Ice Streams D & E in West Antarctica. A low-resolution rendering of the estimated topographic surface for the downstream end of Ice Stream D is shown in Figure 9. The foreground rise is ridge D-E, and the background rise is Siple Dome.

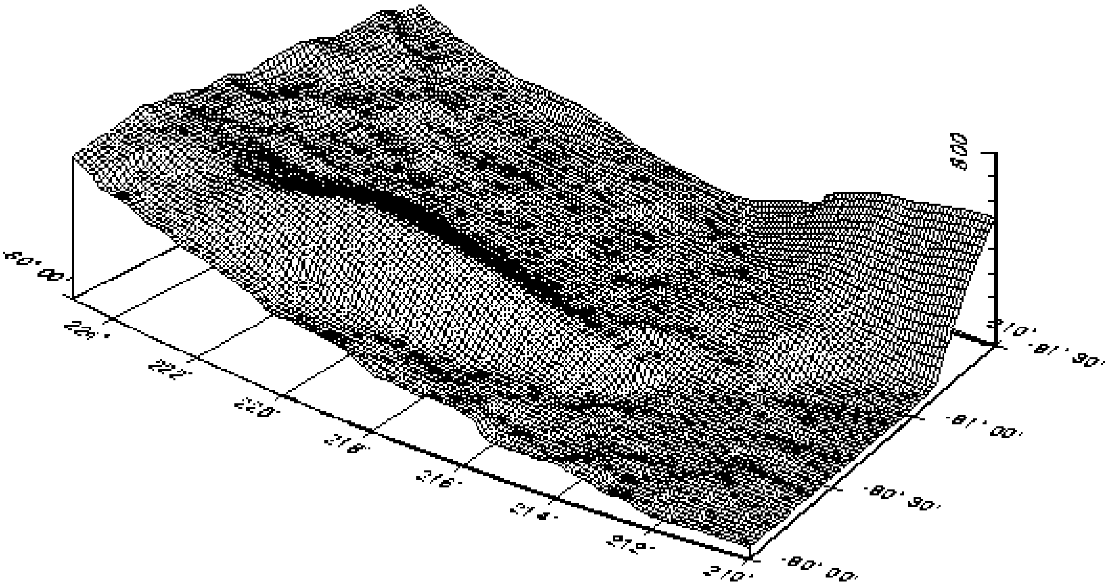

Figure 9: *A topographic estimate of the downstream end of Ice Stream D in West Antarctica.*

Both this topographic estimate and the one in Figure 10 have been produced by the baseline algorithm with the dimple filter algorithm applied.

A topographic estimate for the Pine Island Glacier and Thwaites Glacier region has been produced, and a map of part of the Pine Island catchment area is reproduced in Figure 10.

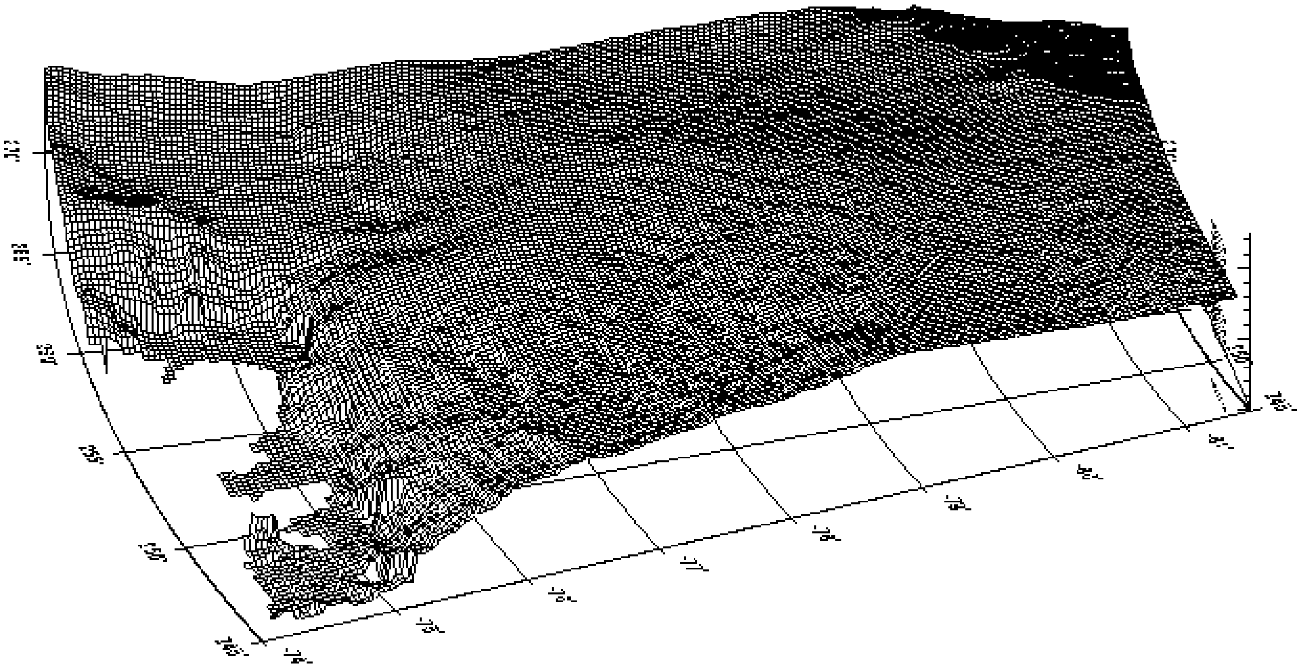

Figure 10: *Gridded topography of a portion of the Pine Island Glacier catchment area.*

A curious characteristic of this topography is the apparent terrace-like quality of the topography. As a check of the reality of this characteristic we have compared the satellite-derived elevations with those calculated by aneroid altimetry along a portion of the 1960-61 oversnow Ellsworth Highland traverse route (Figure 11).

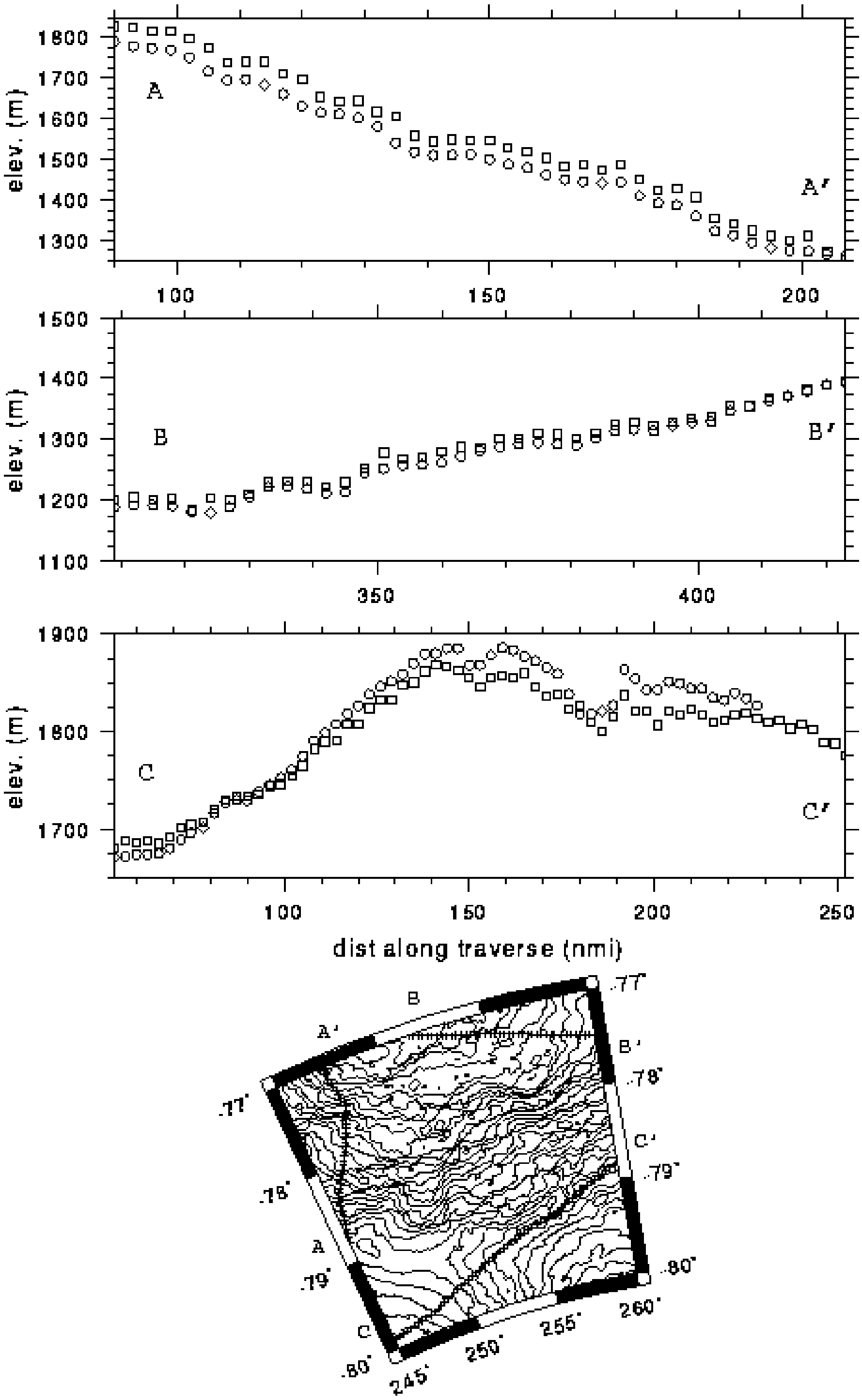

Figure 11: *Comparison of heights derived from satellite altimetry (circles) with those derived from aneroid altimeter measurements on the surface (squares). Aneroid altimeter heights obtained during the 1957-1958 Sentinel traverse (A-A' and B-B') and during the 1960-1961 Ellsworth-Highland traverse (C-C').*

4 Discussion

At this writing we have not yet undertaken a detailed study of the topographic characteristics of the regions shown in Figures 9 and 10. However, we have investigated further the oddly terraced topography in Figure 10, principally to ascertain whether it is a real feature of the ice sheet or an artifact our topographic estimator. That topography is shown in the form of a contour map in Figure 11d, on which segments of the tracks of two oversnow traverses from the IGY (1957-58) and post-IGY (1960-61) years are superimposed.

Elevations on the oversnow traverses were measured every 3 nautical miles by aneroid altimeter, using an interval method that eliminated the effect of temporal changes, but not spatial gradients, in the barometric pressure. Errors of several tens of meters in the absolute surface heights are to be expected, but relative heights over distances of 10 or 20 kilometers should be substantially more accurate than that [Bentley, 1964].

Elevations from the traverses and from the ERS-1 radar altimetry shown in Figure 11d are compared in Figures 11a, b, and c. The abscissas on each plot are distance along the traverse route in nautical miles (the unit used in the traverse navigation). Elevations for the ``Sentinel'' traverse (1957-58) were taken from Bentley and Ostenso (1961); those for the ``Ellsworth-Highland'' traverse (1960-61) are from the second author's unpublished data.

Height estimates along the traverse routes were obtained from the satellite data by interpolating the topographic estimate depicted in figure 10 at the same latitudes and longitudes as the traverse data. Because the satellite altimeter heights are relative to the WGS-84 ellipsoid, while the pressure altimeter data are necessarily relative to the geoid, and because of the errors inherent in the traverse measurements, offsets as large as a few tens of meters between the two sets of profiles are to be expected. Nevertheless, the same short-scale topography should appear on both. We will consider each of the profiles in turn in this regard.

Section AA' is a particularly apt comparison because the track line is at a large angle to the elevation contours and crosses several ``terraces.'' There is indeed close agreement between the two profiles here, with both showing the same alternating steeper and flatter slopes -- e.g. the relatively flat stretches at 110, 126, 143, 170, and 200 n. mi. This profile gives strong support to the reality of the ``terraces.''

Section BB' is less well suited for a comparison because the topography is much more subdued than in the other sections (cf. Figure 11d). Nevertheless, there are several distinct changes in slope between 310 n. mi. and 360 n. mi. that are closely similar on both sets of data. The excellent agreement on the smoother section of the profile, from 360 to 420 n. mi., is also impressive.

The agreement on Section CC' is less impressive at first appearance. There is a fair correspondence on the smooth slope in the first part of the profile(60-140 n. mi.), but it is decidedly poorer from there on. One possible reason for this is that this track runs nearly parallel to the average direction of the contours in a place where the contour lines are close together, so a slight lateral error in traverse navigation (which could be as much as a kilometer) could cause a large elevation effect. Nevertheless, both the traverse and the satellite profiles do show rough, irregular surface topography and several of the same specific features exist, even if they differ in detail: viz. the little valley at 152 n. mi., the broad valley between 175 and 190 n. mi., the steep slope on the edge of that valley at 190 n. mi., and the little valley at 200 n. mi.

Taken all in all, there is little doubt that, in general, the features depicted in Figures 10 and 11d are real characteristics of the ice-sheet surface, not instabilities in the topographic estimation method.

Yet another proof of this is the fact that the ``terraced'' regions coincide with regions of mottled-appearing surface that shows clearly on a satellite image map of the region (Ref.). (That map cannot be reproduced here but the relevant sections will be included in the oral presentation of this paper.)

The cause of the ``terraces'' remains a mystery. It is obvious from a comparison of Figures 9 and 10 that this characteristic is very different from both the fast-flowing ice of ice-stream D (in the surface of which many reflections of the topography of the bed appear) and the nearly stagnant ice of ridge DE, which has the smooth surface characteristic of slow-moving ice. Unfortunately, no detailed map of bed topography exists for much of this region - airborne radar sounding has only been conducted in the more southerly portion [Jankowski and Drewry, 1981]. Farther north there are only seismic soundings at 40- or 50-km intervals along the traverse routes and gravity-based interpolations (which are both inaccurate and broadly smoothing) in between. However, the terraces simply do not look like any form to be expected in the topography of what was once, before the ice sheet formed, the ocean floor. It seems more likely to us that they are the result of some characteristic of the ice dynamics. (T. Hughes (personal communication, 1997) believes that this irregular surface may be result from the first stages of a rapid increase (surge?) in Thwaites Glacier.) Perhaps ice velocities measured by interferometric SAR using the ERS satellites (work currently in progress) will help to solve this intriguing mystery.

5 Conclusions

The baseline algorithm, when fortified with the ``dimple-filter'' and applied to geodetic mission data provides a topographic estimate, that when sampled on a 2km grid appears to be accurate to within a few meters of elevation when applied to the interior of the West Antarctic ice sheet.

References

Bamber, 1994
: Bamber, J. (1994). Ice sheet altimeter processing scheme. *Int. J. of Remote Sens.*, 15(4):925 - 938.

Bentley, 1964
: Bentley, C. R. (1964). The structure of Antarctica and its ice cover. In Odinshaw, H., editor, *Research in Geophysics*, volume 2, pages 335-389. Massachusetts Institute of Technology.

Bentley and Ostenso, 1961
: Bentley, C. R. and Ostenso, N. A. (1961). Glacial and subglacial topography of West Antarctica. *J. of Glac.*, 3(29):882-911.

Brenner et al., 1983
: Brenner, A. C., Bindschadler, R. A., Thomas, R., and Zwally, H. J. (1983). Slope-Induced Errors in Radar Altimetry Over Continental Ice Sheets. *J. of Geophys. Res.*, 88(C3):1617 - 1623.

Jankowski and Drewry, 1981
: Jankowski, E. J. and Drewry, D. J. (1981). The structure of West Antarctica from geophysical studies. *Nature*, 291:17-21.

Martin et al., 1983
: Martin, T. V., Zwally, H. J., Brenner, A. C., and Bindschadler, R. A. (1983). Analysis and retracking of continental ice sheet radar altimeter waveforms. *J. of Geophys. Res.*, 88(C3):1608 - 1616.

Wingham et al., 1993
: Wingham, D., Rapley, C., and Morley, J. (1993). Improved resolution ice sheet mapping with satellite radar altimeters. *EOS, Trans. A.G.U.*, 74(10):113,116.

Zwally et al., 1989
: Zwally, H. J., Brenner, A. C., Major, J., Bindschadler, R. A., and Marsh, J. (1989). Growth of the Greenalnd ice sheet: Measurement. *Science*, 246(4937):1587 - 1591.

About this document ...

Topography estimation in W Antarctica using level 2 radar altimeter data products

The command line arguments were:
latex2html `-split 0 -link 0 -no_navigation -show_section_numbers 00.`

The translation was initiated by Mark Stenoien on Sun Mar 9 14:46:08 CST 1997

...level-2
: The level-2 ERS-1 data product obtained from Hughes STX, consisting of individual altimeter observations, is called an Ice Data Record (IDR). Ice data records are corrected for earth tides and ionospheric and tropospheric refraction and have had precise orbit corrections applied.

...is

Here the height error 5#5 has been approximated by 6#6, where *x* is the distance between the echo point and the grid point.

...many

The maximum number of grid nodes that may be determined by an altimeter datum depends on the spacing of the grid nodes and the spacing of the satellite ground tracks. In cases such as Figures 9 and 10, where 20#20 km grid node spacing and 168-day repeat data are used, we allow each altimeter datum to determine at most 4 grid node heights.

Mark Stenoien
Sun Mar 9 14:46:08 CST 1997